

Design of Achromatic Combined Quadrupole Lens Using the Modified Bell-Shaped Field Distribution Model

Oday A. Hussein^{*}, Fatma N. Gaafer^{**}, Sura A. Obaid^{***}

^{*} Department of Physics, College of Science, Al-Nahrain University, Baghdad, Iraq

^{**} Department of Physics, College of Science, University of Wasit, Wasit, Iraq

^{***} College of Medicine, Al-Nahrain University, Baghdad, Iraq

E-mail: udayalobaidy@yahoo.com

Abstract

The optimization calculations are made to find the optimum properties of combined quadrupole lens consist of electrostatic and magnetic lenses to produce achromatic lens. The modified bell-shaped model is used and the calculation is made by solving the equation of motion and finding the transfer matrices in convergence and divergence planes, these matrices are used to find the properties of lens as the magnification and aberrations coefficients. To find the optimum values of chromatic and spherical aberrations coefficients, the effect of both the excitation parameter of the lens (n) and the effective length of the lens into account as effective parameters in the optimization processing.

Key words

Combined
Quadrupole Lens,
Achromatic Lens,
Modified Bell-Shaped
Model

Article info

Received: May. 2009

Accepted: Sep. 2009

Published: Dec. 2011

تصميم عدسة رباعية مركبة لا لونية باستخدام أنموذج توزيع المجال ذو الشكل الناقوسي – المطور

عدي علي حسين^{*} - فاطمة نافع جعفر^{**} - سرى علاوي عبيد^{***}

^{*} قسم الفيزياء – كلية العلوم – جامعة النهرين

^{**} قسم الفيزياء – كلية العلوم – جامعة واسط

^{***} كلية الطب – جامعة النهرين

الخلاصة

حسابات الأمثلية أجريت لإيجاد أفضل الخواص لعدسة رباعية مركبة مكونة من عدسة كهروسكونية ومغناطيسية وذلك من أجل الحصول على عدسة عديمة الزيغ للوني. الأنموذج الناقوسي المطور لتوزيع الجهد استخدم والحسابات أجريت من خلال حل معادلة الحركة وإيجاد مصفوفات الانتقال للمستويين التقاربي والتباعدي والتي تم استخدامها لإيجاد خواص العدسة مثل التكبير ومعاملات الزيغ. وإيجاد أفضل القيم لمعاملات الزيغ الكروية واللونية تم أخذ تأثيرات تغير كل من عامل التهيح للعدسة وطولها الموجي بنظر الاعتبار كعوامل فعالة للوصول للأمثلية.

Introduction

The quadrupole lenses for focusing charged particle beams is due to the fact that

quadrupole lens systems can converge the beam in all directions, even though the

individual lenses cause the beam to diverge in certain directions [1].

Quadrupole lenses are very suitable for forming a fine linear beam and a spot beam [2]. They are commonly used for focusing electron and ion beams of high energy. An example of such device is the ion implantation [3]. There are many electron and ion optical instruments and devices in which there are advantages in using quadrupole lenses rather than round lenses, such as instruments where strong focusing or astigmatic properties are needed. Among these are the accelerators, electron and mass spectrometers, cathode-ray tubes and devices for correcting aberrations (see for example [4 - 7]).

Electrostatic quadrupole lenses are often preferable to magnetic ones for focusing beams of moderate energy. They are also preferable for dealing with ion beams since the focal length of an electrostatic lens does not depend on the charge to mass ratio as it does for a magnetic lens. It seems that quadrupole lens systems are more sensitive to mechanical defects than round lens [8].

Achromatic quadrupole lens is used to overcome the limitation due to energy spread. These lenses require both magnetic and electrostatic focusing elements [9].

The first order chromatic aberration can be reduced using combined electrostatic and magnetic quadrupole whose excitations are connected by the achromatic condition. This method involves magnetic elements and leads to a complicated construction of the focusing system [10].

In the present work the modified bell-shaped model is used to explain the field distribution of a quadrupole lens [11]:

$$f(z) = 1/[1 + ((z - z_1)/d)^2]^2 \quad \text{at } z > z_1 \quad \dots\dots\dots(1)$$

$$f(z) = 1/[1 + ((z + z_1)/d)^2]^2 \quad \text{at } z > -z_1$$

2. Trajectory of Charged – Particles Beam

The paraxial ray equation in Cartesian coordinates for the charged-particles beam traversing the field of a quadrupole lens is given as follows [12]:

$$x'' + \beta^2 f(z) x = 0 \quad \dots\dots\dots (2)$$

$$y'' - \beta^2 f(z) y = 0 \quad \dots\dots\dots (3)$$

where β is the lens excitation.

The general solution of the second-order linear homogeneous differential equations (2) and (3) can be written respectively in the following matrix form [12]:

$$\begin{pmatrix} x(z) \\ x'(z) \end{pmatrix} = T_c \begin{pmatrix} x_o(z) \\ x'_o(z) \end{pmatrix} \quad \dots\dots\dots (4)$$

$$\begin{pmatrix} y(z) \\ y'(z) \end{pmatrix} = T_d \begin{pmatrix} y_o(z) \\ y'_o(z) \end{pmatrix} \quad \dots\dots\dots (5)$$

where x_o and y_o are the initial displacements from the optical axis in the $x-z$ and $y-z$ planes respectively, and x'_o and y'_o are the initial gradients of the beam in the corresponding planes. The parameter T_c and T_d are the transfer matrices in the convergence plane xoz and the divergence plane yoz respectively and are given by [13] and [14].

$$T_c = \begin{pmatrix} \frac{d \cos(w_c \psi)}{\sin(\psi)} & \frac{d \sin(w_c \psi)}{\sin(\psi)} \\ \frac{[d w_c \sin(\psi) \sin(w_c \psi) + d \cos(\psi) \cos(w_c \psi)]}{\sin^2(\psi)[1 + z^2/d^2]d} & \frac{[d \cos(\psi) \sin(w_c \psi) - d w_c \sin(\psi) \cos(w_c \psi)]}{\sin^2(\psi)[1 + z^2/d^2]d} \end{pmatrix} \quad \dots\dots\dots(6)$$

$$T_d = \begin{pmatrix} \frac{d \cos(w_d \psi)}{\sin(\psi)} & \frac{d \sin(w_d \psi)}{\sin(\psi)} \\ \frac{[d w_d \sin(\psi) \sin(w_d \psi) + d \cos(\psi) \cos(w_d \psi)]}{\sin^2(\psi)[1 + z^2/d^2]d} & \frac{[d \cos(\psi) \sin(w_d \psi) - d w_d \sin(\psi) \cos(w_d \psi)]}{\sin^2(\psi)[1 + z^2/d^2]d} \end{pmatrix} \quad \dots\dots\dots(7)$$

where d is the axial extension of the field and

$$w_c = 1 - \beta^2 d^2 \text{ (convergence plane)...(8)}$$

$$w_d = 1 + \beta^2 d^2 \text{ (divergence plane) ... (9)}$$

and

$$(z - z_L) / d = \cot(\psi) \dots (10)$$

In practice, the length L is the "effective length" which has been found experimentally to be given by [12].

$$L = \ell + 1.1c \dots\dots\dots (11)$$

where ℓ is the electrode length and c is the bore radius which is assumed to be very small. Therefore, the effective length L could be equal to the electrode length ℓ by neglecting the second term of equation (11), i.e. $L \approx \ell$ [12].

Figure (1) shows the trajectories of charged particles beam through combined quadrupole lens in both convergence and divergence planes. From the figure the charged particles in the convergence plane (x-z) deflected toward the optical axis and away from the optical axis in the divergence plane (y-z). i.e. the combined quadrupole lens is astigmatic, and the results coincided with that published by Baranova and Yavor [1].

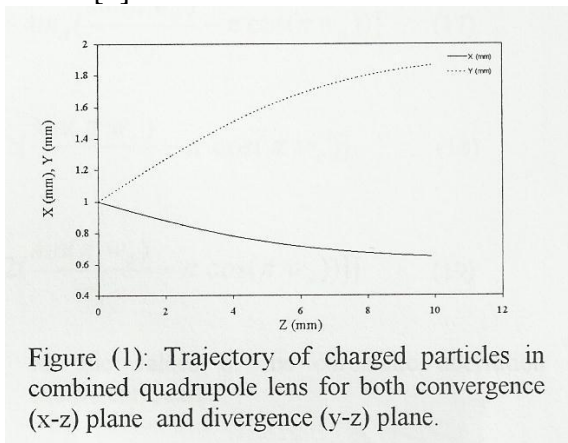


Figure (1): Trajectory of charged particles in combined quadrupole lens for both convergence (x-z) plane and divergence (y-z) plane.

3. Chromatic Aberration

The chromatic aberration coefficients, defined by the following equations [12]:

$$\Delta X(z_i) = M_c (Ccx \alpha + Cmx x_o) \frac{\Delta V}{V} \dots\dots(12)$$

$$\Delta Y(z_i) = M_d (Ccy \gamma + Cmy y_o) \frac{\Delta V}{V} \dots(13)$$

where x_o and y_o are the initial displacements from optical axis in the x-z plane and y-z plane, respectively; α and γ are the image side semi-aperture angles in the x-z and y-z planes, respectively. M_c and M_d are the magnification in both convergence and divergence planes respectively and are given by:

$$M_c = \frac{1}{\frac{d w_c \sin(\psi) \sin(w_c \psi) + d \cos(\psi) \cos(w_c \psi)}{\sin^2(\psi)[1 + (z/d)^2]d} u + \frac{d \cos(w_c \psi)}{\sin(\psi)}} \dots\dots (14)$$

$$M_d = \frac{1}{\frac{d w_d \sin(\psi) \sin(w_d \psi) + d \cos(\psi) \cos(w_d \psi)}{\sin^2(\psi)[1 + (z/d)^2]d} u + \frac{d \cos(w_d \psi)}{\sin(\psi)}} \dots\dots (15)$$

where u is the object distance.

The coefficients of chromatic aberration in a modified bell-shaped model of the field distribution are given by [12]:

$$\frac{Ccx}{d} = -\frac{n-1}{8} \frac{\beta^2 d^2}{\sin(\pi w_c)^2} \left[\left(\frac{\sin(2\pi w_c)}{w_c} - 2\pi \right) (m_c^2 + 1) + 4m_c \left(\frac{\sin(\pi w_c)}{w_c} - \pi \cos(\pi w_c) \right) \right] \dots\dots\dots(16)$$

$$\frac{Ccy}{d} = \frac{n-1}{8} \frac{\beta^2 d^2}{\sin(\pi w_d)^2} \left[\left(\frac{\sin(2\pi w_d)}{w_d} - 2\pi \right) (m_d^2 + 1) + 4m_d \left(\frac{\sin(\pi w_d)}{w_d} - \pi \cos(\pi w_d) \right) \right] \dots\dots\dots(17)$$

$$Cmx = \frac{n-1}{8} \frac{\beta^2 d^2 f_c}{w_c^2 d} \left[\left(\frac{\sin(2\pi w_c)}{w_c} - 2\pi \right) m_c + 2 \left(\frac{\sin(\pi w_c)}{w_c} - \pi \cos(\pi w_c) \right) \right] \dots\dots (18)$$

$$Cmy = -\left[\frac{n-1}{8} \frac{\beta^2 d^2 f_d}{w_d^2 d} \left[\left(\frac{\sin(2\pi w_d)}{w_d} - 2\pi \right) m_d + 2 \left(\frac{\sin(\pi w_d)}{w_d} - \pi \cos(\pi w_d) \right) \right] \right] \dots\dots (19)$$

where $n = \frac{\beta e^2}{\beta^2} = \frac{\beta e^2}{\beta m^2 - \beta e^2} \dots\dots (20)$

and $d = \frac{2L}{\pi}$, β_e and β_m are the excitation of electric and magnetic lenses respectively.

The calculations of finding the achromatic lens is made via taking the effect of both the excitation parameter of the lens (n) and the effective length of the lens into account as effective parameters in the optimization processing. Two effective lengths of the lens are investigated ($L_1=0.9$ mm and $L_2=1$ mm) and the chromatic aberration coefficients are found in both convergence and divergence plane.

The relation between the chromatic aberration coefficients and the relative excitation parameter (n) is shown for both convergence and divergence planes in figures (2) to (5). Figure (2) shows the relation between the chromatic aberration coefficient C_{cx}/L and the relative excitation parameter (n). In general, the chromatic aberration coefficient C_{cx}/L is decreasing as the relative excitation parameter (n) increasing and the effective length of lens L_2 has values of the chromatic aberration coefficient C_{cx}/L greater than that of L_1 and this increasing of the difference increases as the relative excitation parameter (n) increase. In the small values of the excitation parameter (n) the peak is found for the values of the chromatic aberration coefficient C_{cx}/L .

The same general behavior is found for the chromatic aberration coefficient of change of magnification C_{mx} as is shown in figure (3), where the value of the chromatic aberration coefficient of change of magnification C_{mx} decreases as the relative excitation parameter (n) increases.

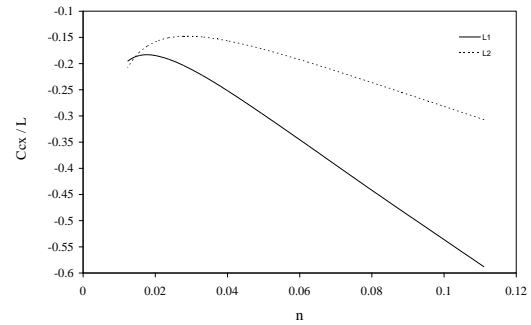


Fig. (2): The relative chromatic aberration coefficients as a function of relative excitation parameter (n) for the combined quadrupole lens in convergence plane for the effective lengths of lens $L_1=0.9$ mm and $L_2=1$ mm.

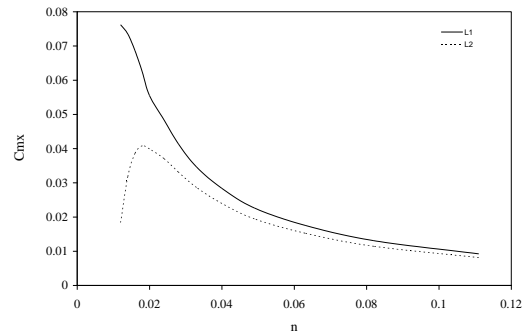


Fig. (3): The relative chromatic aberration coefficients of change of magnification as a function of relative excitation parameter (n) for the combined quadrupole lens in convergence plane for the effective lengths of lens $L_1=0.9$ mm and $L_2=1$ mm.

For the divergence plane, the results are shown in figures (4) and (5). From figure (4) the calculations appear that the the chromatic aberration coefficient C_{cy}/L is increasing as the relative excitation parameter (n) is increasing and the values of the effective length of lens L_2 (0.9mm) are lower than that of L_2 (1mm) and the increasing in the values of the chromatic aberration coefficient C_{cy}/L is faster for L_2 than L_1

The same general behavior of chromatic aberration coefficient change of magnification C_{my} is found as shown in figure (5), but the effective length $L_1(0.9\text{mm})$ gives the values of the chromatic aberration coefficient lower than that of $L_2(1\text{mm})$.

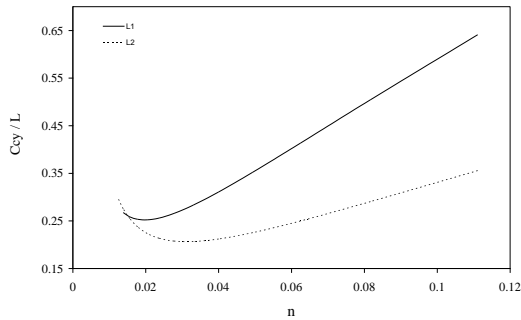


Fig. (4): The relative chromatic aberration coefficients as a function of relative excitation parameter (n) for the combined quadrupole lens in divergence plane for the effective lengths of lens $L_1=0.9\text{mm}$ and $L_2=1\text{mm}$

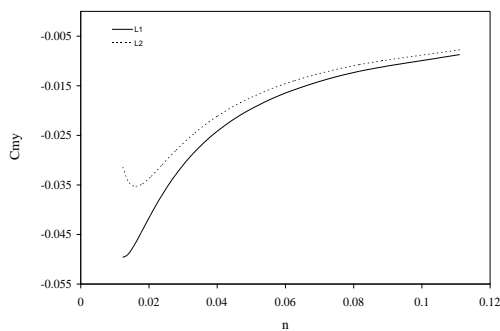


Fig. (5): The relative chromatic aberration coefficients change of magnification as a function of relative excitation parameter (n) for the combined quadrupole lens in divergence plane for the effective lengths of lens $L_1=0.9\text{mm}$ and $L_2=1\text{mm}$.

4. Spherical Aberration

The spherical aberration coefficients, defined by the following equations [12]:

$$\Delta X(z_i) = M_c (C_{30} \alpha^3 + C_{12} \alpha \gamma^2) \dots (21)$$

$$\Delta Y(z_i) = M_d (D_{03} \gamma^3 + D_{21} \alpha^2 \gamma) \dots (22)$$

The coefficients C characterize the aberration in convergence plane, and D in the divergence plane.

The coefficients of spherical aberration in a modified bell-shaped model of the field distribution are given by [15]:

$$\frac{C_{30}}{d} = \frac{1}{32 \sin^4 \psi_0} [(w_c^2 - 1)(w_c^2 + 3) \frac{\pi}{w_c^5} + \frac{2(7 - w_c^2)}{4w_c^2 - 1} (\sin 2\psi_0 - \sin 2\psi_1) + (2 - 2n + 3n^2)(w_c^2 - 1) \frac{\pi}{w_c^5} - \frac{2}{4w_c^2 - 1} (\sin 2\psi_0 - \sin 2\psi_1)] \dots (23)$$

$$\frac{C_{12}}{d} = \frac{1}{32w_d^2 \sin^4 \psi_0} \{ [-4(1 - \cos 2\pi \frac{w_d}{w_c}) \sin 2\psi_1 + w_d(1 - \cos 2\psi_1) \sin 2\pi \frac{w_d}{w_c} + 3(w_c^2 - 1)[-2(w_c^2 - 1) \frac{\pi}{w_c^3} + \frac{1}{w_c^2 - 1} [-\frac{w_d^2(w_c^2 w_d^2 + 2)}{4w_c^2 w_d^2 - 1} \sin 2\psi_0 + (w_d^2 + 3) \sin 2\psi_1 + \frac{3w_d^2 + 1}{2w_d} \sin 2\pi \frac{w_d}{w_c}] - \frac{3}{4w_c^2 w_d^2 - 1} [(4w_d^2 - 1) \sin 2\psi_1 \cos 2\pi \frac{w_d}{w_c} + w_d(2w_d^2 + 1) \cos 2\psi_1 \sin 2\pi \frac{w_d}{w_c}] + (2 + 2n - n^2)(w_c^2 - 1) \frac{\pi}{w_c^3} - \frac{4w_d^2(w_c^2 - 1)}{4w_c^2 w_d^2 - 1} \sin 2\psi_0 + \sin 2\psi_1 - \frac{1}{2w_d} \sin 2\pi \frac{w_d}{w_c} - \frac{1}{4w_c^2 w_d^2 - 1} [(4w_d^2 - 1) \sin 2\psi_1 \cos 2\pi \frac{w_d}{w_c} + w_d(2w_d^2 + 1) \cos 2\psi_1 \sin 2\pi \frac{w_d}{w_c}]] \} \dots (24)$$

$$\frac{D_{03}}{d} = \frac{w_c^2 - 1}{32w_d^4 \sin^4 \psi_0} \{ -\frac{1}{3} [2(2 + n)w_d(1 - \cos 2\psi_1)(1 - \cos 2\pi \frac{w_d}{w_c}) \sin 2\pi \frac{w_d}{w_c} + (4 - n)(\cos 4\pi \frac{w_d}{w_c} - 4 \cos 2\pi \frac{w_d}{w_c} + 3) \sin 2\psi_1 - (w_d^2 + 3) \frac{\pi}{w_c} + \frac{2w_d^4(5 + w_c^2)}{(w_c^2 - 1)(4w_d^2 - 1)} \sin 2\psi_0 + \frac{1 + w_c^2}{2} \sin 2\psi_1 + \frac{2}{w_d} \sin 2\pi \frac{w_d}{w_c} - \frac{w_c^2 - 1}{4w_d} \sin 4\pi \frac{w_d}{w_c} - \frac{2}{w_c^2 - 1} [(w_d^2 + 1) \sin 2\psi_1 \cos 2\pi \frac{w_d}{w_c} + 2w_d \cos 2\psi_1 \sin 2\pi \frac{w_d}{w_c}] - \frac{1}{2(4w_d^2 - 1)} [(5w_d^2 + 1) \sin 2\psi_1 \cos 4\pi \frac{w_d}{w_c} + 2w_d(w_d^2 + 2) \cos 2\psi_1 \sin 4\pi \frac{w_d}{w_c}] + \frac{1}{3} (2 - 2n + 3n^2)(w_c^2 - 1) \frac{3\pi}{w_c} + \frac{6w_d^4}{(w_c^2 - 1)(4w_d^2 - 1)} \sin 2\psi_0 + \frac{3}{2} \sin 2\psi_1 - \frac{2}{w_d} \sin 2\pi \frac{w_d}{w_c} + \frac{1}{4w_d} \sin 4\pi \frac{w_d}{w_c} - \frac{2}{w_c^2 - 1} (\sin 2\psi_1 \cos 2\pi \frac{w_d}{w_c} + w_d \cos 2\psi_1 \sin 2\pi \frac{w_d}{w_c}) - \frac{1}{2(4w_d^2 - 1)} (\sin 2\psi_1 \cos 4\pi \frac{w_d}{w_c} + 2w_d \cos 2\psi_1 \sin 4\pi \frac{w_d}{w_c}) \} \dots (25)$$

$$\frac{D_{21}}{d} = \frac{C_{12}}{d} - \frac{1}{8w_d^2 \sin^4 \psi_0} [(1 - \cos 2\pi \frac{w_d}{w_c}) \sin 2\psi_1 + w_d(1 - \cos 2\psi_1) \sin 2\pi \frac{w_d}{w_c}] \dots (26)$$

The optimization calculations for spherical aberration coefficients in both convergence and divergence plane are made to show the effect of changing the excitation parameter and the effective lengths of lens on the spherical aberration coefficients.

The results of the optimization calculations for the spherical aberration coefficients for the convergence plane are shown in figures (6) and (7). In figure (6), the relation between the spherical aberration coefficient C_{30}/L is plotted as a function of the relative excitation parameter (n) for two values of the effective length of the lens L1(0.9mm) and L2(1mm). The results show that the spherical aberration coefficient C_{30}/L increases as the relative excitation parameter (n) is increasing. The effective length of the lens L2(1mm) has values of spherical aberration coefficient lower than that of L1(0.9mm) at lower values of the relative excitation parameter (n), while the values of the chromatic aberration coefficient for the two values of effective length of the lens is overlaped at the relative excitation parameter (n) equal to 0.07 and the opposite behavior is found beyond this region .

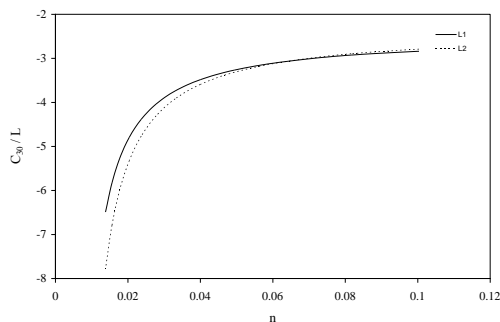


Fig. (6): The relative spherical aberration coefficients C_{30}/L as a function of relative excitation parameter (n) for the combined quadrupole lens in convergence plane for the effective lengths of lens L1=0.9mm and L2=1mm.

From figure (7) the spherical aberration coefficient C_{12}/L has inverse relation with the relative excitation parameter (n) and the calculations show that the effective length of the lens L2 has the better results in comparison with L1.

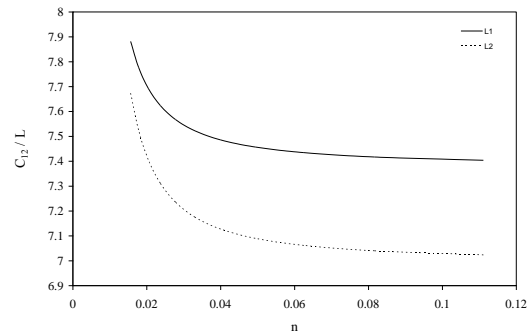


Fig. (7): The relative spherical aberration coefficients C_{12}/L as a function of relative excitation parameter (n) for the combined quadrupole lens in convergence plane for the effective lengths of lens L1=0.9mm and L2=1mm.

The calculations of the divergence case are shown in figures (8) and (9). Figure (8) gives the relation between spherical aberration coefficient D_{30}/L and relative excitation parameter (n), this coefficient has two opposite behavior for two effective lengths of the lens at the low values of the relative excitation parameter while the two curves has the same behavior at the region of high value of relative excitation parameter (n).

The relation between spherical aberration coefficient D_{21}/L and relative excitation parameter (n) is shown in figure (9), this relation is found to be inversely. In both cases of the divergence plane the effective length of lens L1 gives the optimum results with respect to another effective length of lens L2.

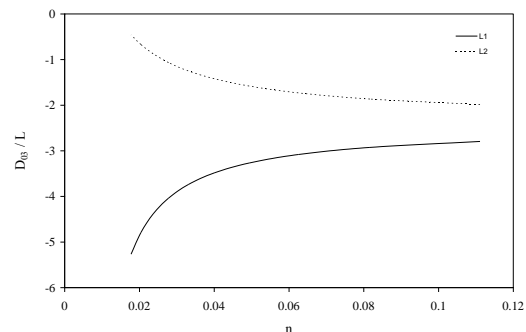


Fig.(8): The relative spherical aberration coefficients D_{30}/L as a function of relative excitation parameter (n) for the combined quadrupole lens in divergence plane for the

effective lengths of lens $L_1=0.9\text{mm}$ and $L_2=1\text{mm}$.

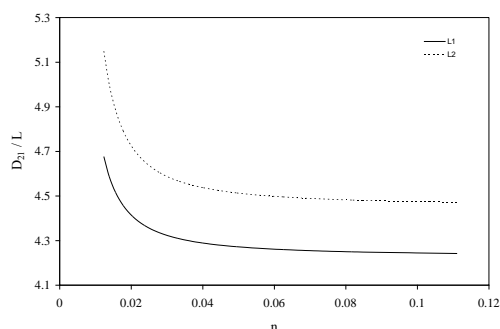


Fig. (9): The relative spherical aberration coefficients D_{21}/L as a function of relative excitation parameter (n) for the combined quadrupole lens in divergence plane for the effective lengths of lens $L_1=0.9\text{mm}$ and $L_2=1\text{mm}$.

6. Conclusions

1- From the calculations, it appears that the modified bell-shaped model can be used to represent the axial field distribution of the combined quadrupole lens to find the optimum design of the achromatic lens and the excitation parameter of the lens (n) and the effective length of the lens (L) can be used as effective parameters to reduced the values of the aberration coefficients where:

a-In some cases the lower values of the excitation parameter of the lens (n) give the best values of the aberration coefficients as: C_{cx}/L , C_{my} and C_{30}/L while the large values of the excitation parameter of the lens (n) give optimum values in the another cases as: C_{cx}/L , C_{mx} , C_{12}/L and C_{21}/L .

b-In some cases the lower value of the effective length of the lens L_1 gives the best values of the aberration coefficients as: C_{cx}/L , C_{my} , D_{03}/L and D_{21}/L , while the large value of the effective length of the lens L_2 gives the best values of aberration coefficients at the C_{30}/L , C_{12}/L , C_{cy}/L and C_{mx} .

According to the above results, the designer can choose the values of the excitation parameter of the lens (n) and

the effective length of the lens (L) to reach a favorable design.

2- From the calculations one can find the negative values of the aberration coefficients, therefore, the designer can use the combined quadrupole lens with these conditions, as a corrector element in the optical system to reduced the total aberration of the system.

References

- [1] L.A. Baranova and S.Ya. Yavor: Sov. Phys. – Tech. Phys. **29** (1984) No. 8, 827.
- [2] S. Okayama: SPIE, Electron-beam, X-ray, and Ion-beam Technology: Submicrometer Lithographies. VIII **1089** - 74 (1989).
- [3] L.A. Baranova and F.H. Read: Optik **109** (1998) No. 1, 15.
- [4] H. Shimizu, F.J. Currell, S. Ohtani, E.J. Sokell, C. Yamada, T. Hirayama, and M. Sakurai: Rev. Scie. Instr. **71** (2000) No. 2, 681.
- [5] L.P. Ovsyannikova and T.Ya. Fishkova: Technical Physics. **46** (2001) No. 5, 601.
- [6] H. Rose: Microsc. Microanal., **9** (2003) 32.
- [7] H. Rose and W. Wan: (2005), Aberration correction in electron microscopy, IEEE, Proceedings of 2005 Particle Accelerator Conference, Knoxville, Tennessee.
- [8] L.A. Baranova and F.H. Read: Optik, **112** (2001) 3, 131.
- [9] L.R. Harriott, W.L. Brown, and D.L. Barr: J. Vacu. Scie. and Tech. A. **8** (1990) No.4, 3279.
- [10] L.A. Baranova and F.H. Read: International Journal of Mass Spectrometry, **189** (1999), 19.
- [11] P.W. Hawkes: Optik, **23** (1965/1966), 145.
- [12] P.W. Hawkes: Quadrupole in electron lens design, Advances in Electronics and Electron Physics, (Academic Press, New York and London, 1970) 1st ed., 123.
- [13] J.D. Larson: Nucl. Instrum. Meth. **189** (1981), 71.
- [14] M. Szilagy: Electron and ion optics (Plenum Press, New York, 1988), 2nd ed., p. 539.
- [15] T.Ya. Fishkova, L.A. Baranova, and S.Ya. Yavor: Sov. Phys. – Tech. Phys. **13** (1968), 520.